ASSESSING THE ABILITY TO DETECT INVASIVE PLANT SPECIES USING DRONE-BASED LEAF-SCALE VISIBLE AND NEAR-INFRARED IMAGING SPECTROSCOPY

Kelsey Huelsman
Advisor Howard Epstein
University of Virginia

Abstract

Controlling the spread of invasive plant species requires extensive ecosystem monitoring. Drones provide data with high spatial resolution and coverage, making them an increasingly popular means to observe ecosystems, including invasive plant species monitoring. Spectroscopic images were collected during the 2020 growing season at Blandy Experimental Farm in northwestern Virginia using a DJI Matrice 600 drone equipped with an imaging spectrometer. Spectroscopic data, which indicates plant chemical and structural properties, should vary among species, but it is not known whether the very fine spatial resolution of data provided by UAV is beneficial or detrimental to the process of differentiation. This project examines whether spectral signals from individual pixels can be utilized to detect autumn olive and whether spectral variability impedes its detection. Using two different models from spectroscopic data collected in April and June, intra-individual and intra-specific variability of autumn olive do not impede the ability to differentiate autumn olive, and individuals can be best detected using complex models in either June or April, with the most accuracy in June. Using a simpler model for detection in June also yielded accurate results and demonstrates potential for broader, open access applications.

Introduction

Globally, invasive plants pose significant threats to natural ecosystems (Gurevitch and Padilla, 2004) and biodiversity (Gaertner et al., 2009; Kimothi and Dasari, 2010; Peerbhay et al., 2016). Across the state of Virginia, invasive, non-native plants are radically altering natural environments by inhibiting the growth of native species upon which native wildlife and insects depend. These widespread changes in species composition also have broader impacts on soil chemistry and forest canopies, with feedbacks on dynamics of carbon, nutrients, water, and energy.

Land managers are making concerted efforts to control the spread of invasive plant species, a task that demands extensive ecosystem monitoring. Data that provide information about spatial patterns and trends of invasive plants is essential to ecosystem monitoring. Traditional approaches to ecosystem observation and monitoring are satellite-based and ground-based. Each approach, however, has caveats: remotely sensed satellite imagery covers large areas but cannot provide fine-scale details, while ground surveying, despite its ability to provide fine-scale details, is labor intensive, and only partially surveys broad areas. Unmanned aerial vehicles (UAVs, or drones) provide data on an intermediate scale, with much higher spatial resolution than satellite data and with more spatial coverage than ground surveys. As UAVs merge the benefits of more traditional satellite-based and ground-based monitoring, they are becoming an increasingly popular means to observe ecosystems, including invasive plant species monitoring.

In addition to the spatial resolution limitations of most traditional satellite-based monitoring, there are also spectral limitations. Much of the remotely sensed data provided by satellite is multispectral, consisting of 4 to 20 discrete spectral bands. Spectroscopic imaging, which includes a large number of narrower, contiguous bands, provides much more detailed spectral information (Chance et al., 2016; Kaufmann et al., 2008). Spectral reflectance signatures provided by spectroscopy are impacted by differences in biophysical and biochemical characteristics of plants (Matongera et al., 2016), including: pigments (Mahlein et al., 2010; Xiao et al., 2014); plant moisture and vegetation stress (Thenkabail et al., 2014); leaf N, P, and/or K (Asner and Martin, 2008; Chance et al., 2016; Mutanga et al., 2004; Thenkabail et al., 2014); chlorophyll (Asner and Martin, 2008; Chance et al., 2016; Thenkabail et al., 2014); and anthocyanins and carotenoids (Blackburn, 2007). Because UAV flights can take place readily at multiple points in the growing season, phenological differences in these features among species can aid in differentiation (Castro-Esau et al., 2006).

Thus, spectroscopic data, which serve as an indication of plant chemical and structural properties, vary within and across ecosystems (Martin and Aber, 1997; Ustin et al., 2004). With current understanding of plant chemical and structural properties, spectroscopy can be used not only to detect general assemblages of plants (Hochberg et al., 2015; Sanchez-Azofeifa et al., 2013; Schmidt and Skidmore, 2003) but also to differentiate species (Clark et al., 2005; Cochrane, 2000). Imaging spectroscopy has been used to identify invasive plant species (Aneece and Epstein, 2017; Asner and Vitousek, 2005; Asner and Martin, 2008; Castro et al., 2004; Chance et al., 2016; Kganyago et al., 2017; Skowronek et al., 2017), using both airborne and handheld spectrometers. Using spectroscopic sensors in concert with UAVs is a relatively new application for these technologies. Whereas a few drone-based studies have been successful in identifying individual plant species, this has been often been accomplished with traditional photography or in large monocultures where the target plant is easily distinguished from the surrounding vegetation. This is the first effort to identify and map invasive plant species using this approach within heterogeneous vegetation communities of the northern Blue Ridge region in Virginia.

Though the benefits of field spectroscopy in classification of plant communities are clear, it is not known whether the very fine spatial resolution of data provided by UAV is beneficial or detrimental to the process of differentiation. Smaller pixel size overcomes the challenge of averaged spectral properties of large pixel sizes over heterogeneous landscapes (Cardina et al., 1997; Carson et al., 1995; Hamilton et al., 2006). Detection of invasive plant species is likely improved by the fine spatial resolution a UAV can achieve, as it does not require large and homogeneous infestation stands. Because UAVs provide spectroscopic imagery with much higher spatial resolution than fixed-wing aircrafts and satellites, it is essential to understand the mechanisms that allow for detection of target invasive plant species within these fine resolution images.

According to the spectral variation hypothesis, spectral variations in remotely sensed images indicate species richness and habitat heterogeneity, which represents the capacity for more species to coexist. Rocchini et al. (2004) and Palmer et al. (2002) used multispectral images to estimate species richness and both found a significant relationship between spectral heterogeneity and species richness. Although spectral signatures vary among plant species and spectral variation is associated with higher diversity, spectral signatures can also vary within individual plant species. For example, Aneece & Epstein (2017) found that of all 50 nm sections of the visible-to-near-infrared spectral profile, 550-599 nm and 650-699 nm sections were detrimental to species identification using field spectroscopy. This is likely due to a higher intra-specific variability than inter-specific variability in those portions of spectra.

Although others have successfully differentiated these invasive plant species using spectroscopy, all were done either in the lab or via *in situ* measurements near the ground; none utilized imagery collected via UAV. Because this is a novel approach to the differentiation plant species in a heterogeneous vegetation community, several questions must be answered to determine how to best accurately detect invasive plant species. Because the fine spatial resolution of data collected by UAV may potentially be detrimental to the process of differentiation, it is essential to examine variability within and among individuals in collected images. Inspired by these gaps in understanding, this project answers the following research questions:

(1) Do intra-individual and intraspecific variability of target invasive plant species impede the ability to differentiate species?
(2) Can the spectral signal from individual pixels be used to effectively detect target invasive plant species in an image?

Methods

Study Site & Data Collection

Spectroscopic images were collected during the 2020 growing season at Blandy Experimental Farm (BEF), a biological field station owned by the University of Virginia. It is located in the Shenandoah Valley in northwestern Virginia

(39.06ºN, 79.07ºW). At 190 m elevation, BEF has a mean annual precipitation of 975 mm, a mean annual temperature of 12ºC and a mean July high temperature of 31.5ºC. It contains 80 ha of old fields in various stages of succession (Bowers, 1997).

Aerial spectroscopic images were collected using a DJI Matrice 600 drone equipped with a high-precision GPS system and an imaging spectrometer (Nano-Hyperspec, Headwall Photonics, Bolton, MA). Data collection took place over two 1-ha fields, which were chosen based on their abundance of invasive plants. The fields are approximately 20-25 years in age and are on low-relief topography.

Figure 1. Locations of fields in which spectroscopic data were collected during the 2020 growing season. The training field and testing field are shown in green and blue, respectively.

The field used to produce a model for invasive plant detection (green polygon in Figure 1; Figure 2A) contains abundant invasive shrubs, including *Elaeagnus umbellata* (autumn olive) and *Rhamnus davurica* (buckthorn) within a heterogeneous matrix of forbs, graminoids, shrubs, and trees (including the invasive tree of heaven, *Ailanthus altissima*). *Celastrus orbiculatus* (Oriental bittersweet) is also present in the tree and shrub canopies of a few individuals. The field used to test the accuracy of the model (blue polygon in Figure 1; Figure 2B) contains abundant invasive shrubs, including *Elaeagnus umbellata* (autumn olive), *Rhamnus davurica* (buckthorn), *Lonicera mackii* (bush honeysuckle) within a heterogeneous matrix of forbs, graminoids, shrubs, and trees, but with more prevalent trees and shrubs than the other field. *Celastrus orbiculatus* (Oriental bittersweet) and *Lonicera japonica* (Japanese honeysuckle) are present in the tree and shrub canopies of a few individuals.

Flight plans over each field were created using Universal Ground Control Software (UgCS), in which the UAV would fly in straight lines at a consistent height of 48 m above the ground in order to obtain images with 3 cm pixels that could later be pieced together to form a larger image. The imaging spectrometer was programmed to capture images along the flight plan using HyperSpec III software (Headwall Photonics, Bolton, MA). Images were collected midday between 10h and 15h under consistent sky conditions at multiple points during the growing season, with higher

Figure 2. A. The field utilized to train the detection algorithm is about 20 years in age and contains abundant invasive shrubs, including *E. umbellata* (pictured on the left) and *R. davurica*. B. The field utilized to test the detection algorithm is about 25 years in age and contains abundant invasive shrubs, including *E. umbellata*, *R. davurica* (pictured in the foreground), and *Lonicera mackii*.

frequency during transitional periods of early season leaf-out and fall senescence (approximately every two weeks from early April through mid-June and from early October to mid-November; approximately every four weeks from mid-June to mid-September).

Collected spectroscopic images were adjusted for incoming and scattered solar radiation using a sampled dark reference at the time of flight and a reference tarp located in the flight scene, respectively. Using HyperSpec III software, terrain and perspective effects were removed using a digital elevation model provided by the US Geological Survey, and a mosaic of multiple images was created.

<u>Data Analysis</u>

Though spectroscopic data were collected at multiple points in the growing season, this preliminary analysis focuses on only two dates: April 15 and June 8 and the detection of one species: *E. umbellata* (autumn olive). 15 well-lit and representative pixels were selected for spectral sampling from individuals of known identities that were present and with foliage in images of each field on each date. A variety of tree and shrub species are present in the field used to develop a detection algorithm, including *Ailanthus altissima* (tree of heaven), *Rhamnus davurica* (Dahurian buckthorn), *Elaeagnus orbiculate* (autumn olive), *Gleditsia triacanthos* (honey locust), *Maclura pomifera* (osage orange), *Juniperus virginiana* (eastern red cedar), *Pinus virginiana* (Virginia pine), *Symphoricarpos orbiculatus* (coralberry), *Galium verum* (yellow bedstraw), and *Rubus spp.* (raspberry species), Catalpa bignonioides (catalpa), and *Phytolacca americana* (pokeweed).

As a preliminary approach to assessing whether variability within species impedes differentiation and detection, mean spectra were calculated for each species, along with a 95% confidence interval for the mean.

Spectral signatures collected from the training field images were then recoded as the species of interest (“olive”) and all other species (recoded as “not olive”) and were analyzed using a partial least squares discriminatory analysis (PLS-DA), which classifies individuals into differing groups using reflectance at various wavelengths. The use of a PLS-DA, which classifies individuals into different groups using their reflectances at various wavelengths, can not only be used to develop a trained classification system but also can elucidate patterns of inter- and intra-specific variability.

Species recoded as “olive” and “not olive” were recoded as 1s and 0s, in order to utilize a probability approach in the model (1s represent 100% probability that a pixel is olive, while 0s represent a 0% probability that a pixel is olive). The training dataset was split into 70% to develop a model and 30% to validate it.

Two approaches to classification were used. The first, a simple linear model, used individual bands that loaded heavily in the PLS-DA. The initial model included bands from all regions that loaded heavily, then variables were removed individually based on collinearity and parsimony (Variance Inflation Factors and Akaike Information Criterion of each variable). Once a model was chosen, it was validated on the remaining training data, and a threshold for probability was chosen as 80%, above which a pixel would be classified as olive and below which it would be classified as not olive. This threshold was chosen as an adequate confidence level as well as one that accurately categorized pixels.

Once a detection model and probability threshold were finalized, the algorithm was tested for accuracy on the second field in which data were collected. Pixels that obtained a probability of 80% or higher were classified as autumn olive, and pixels with a probability below 80% were classified as not autumn olive. If at least half of pixels within an individual tree or shrub were classified as autumn olive, that individual was classified as autumn olive.

The second approache to classification used PLS-R to create a more complex model, which used all wavelengths rather than a select few to determine the probability that a pixel was autumn olive. The accuracy of the PLS-R model was compared to the simple linear model in order to evaluate the efficacy of less computationally demanding models or the need for complex models for detection.

Results

In April, autumn olive (light green curve, Figure 3A) differs from other plant species in the blue region of its spectrum. The mean reflectance as well as its 95% confidence interval is greater than other plants in blue bands with no overlap with other plants. Spectra extracted from pixels of autumn olive individuals in April also have high reflectance in red bands, in the red edge, and in NIR bands, though the 95% confidence intervals overlap with some species (buckthorn, coralberry, pine, and blackberry; Figure 3A).

In June, the spectral signal of autumn olive (light green curve, Figure 3B) is not as noticeably different in the same regions. Reflectance in blue bands remains high, but the 95% confidence interval of the mean overlaps with other species (cedar, tree of heaven, and others). Its reflectance in the red edge region, though not among the highest or lowest of all species, is still relatively differentiable; the 95% confidence interval of the mean in the red edge overlaps with only pokeweed, coralberry, and osage orange.

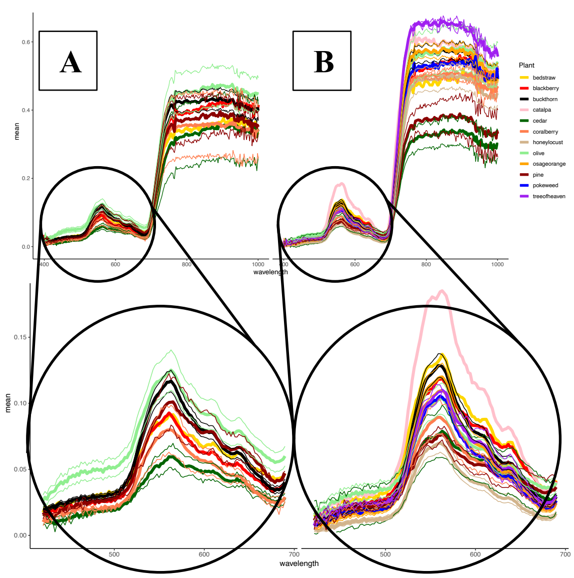

Figure 3. Average reflectance (bold line) for each species over all wavelengths in April (A) and June (B), with 95% confidence interval of the mean (thinner lines above and below) for each species. The visible portion of the spectrum is shown enlarged below each full signature for more detail.

The partial least squares discriminatory analysis (PLS-DA) of spectroscopic data collected in April shows promise for discrimination among autumn olive and other plants. Autumn olive pixels tend to cluster in the component space negatively for component 1 and positively for component 2 (Figure 4A). Loading values of component 1 are highly negative in the blue region (around 470 to 500 nm) and less so in the red region (around 690 nm; Figure 4B). Loading values of component 2 are somewhat positive in the blue region and red region, but loading values at the red edge (710 nm) load heavily in the negative direction (Figure 4C).

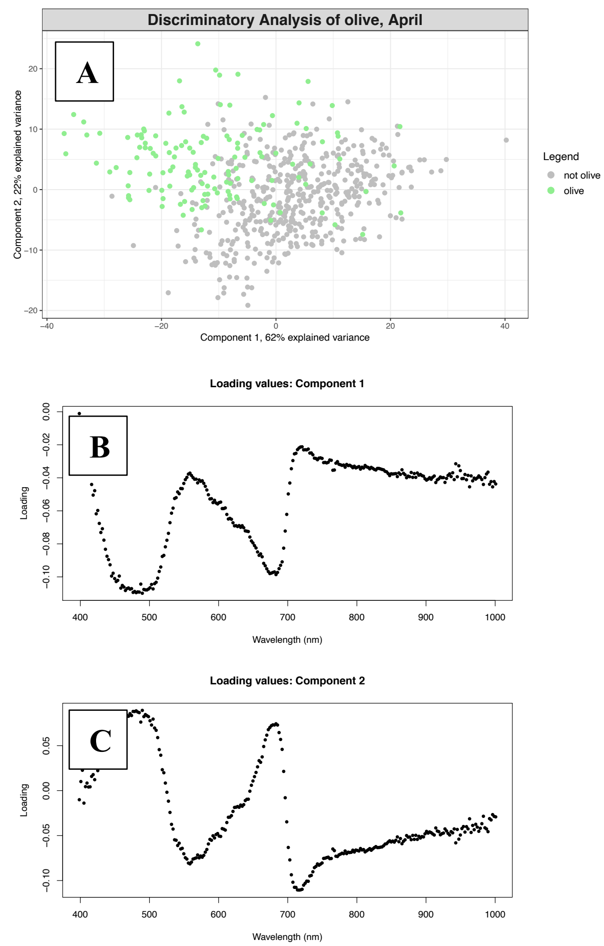

Figure 4. PLS-DA for autumn olive pixels compared to pixels of all other species in April. Panel A shows where autumn olive pixels tend to cluster in the component space, and Panels B and C show the loading values (importance) of each wavelength in each component. Values farther from zero are more important.

The PLS-DA for spectroscopic data collected in June also shows promise for discrimination among autumn olive and other plants. Autumn olive pixels tend to cluster in the component space positively for component 1 and positively for component 2 (Figure 5A). Like loading values in the April PLS-DA, loading values of component 1 are highly positive in the blue region (around 470 to 500 nm) and in the red region (around 690 nm; Figure 5B). Loading values of component 2 are highly negative at the red edge (around 710 nm) as well as in the green region (around 550 nm) (Figure 5C).

Bands that loaded heavily in the PLS-DA components were used to produce the algorithms to

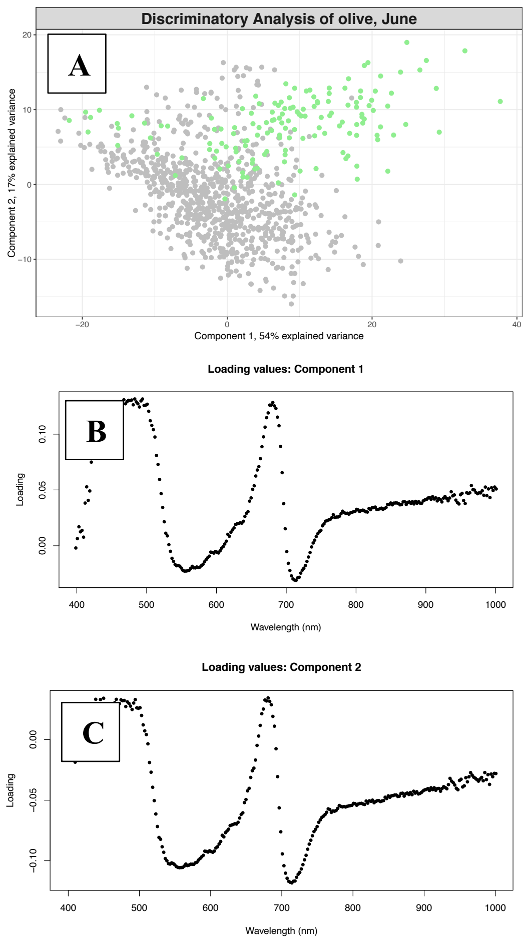

Figure 5. PLS-DA for autumn olive pixels compared to pixels of all other species in June. Panel A shows where autumn olive pixels tend to cluster in the component space, and Panels B and C show the loading values (importance) of each wavelength in each component. Values farther from zero are more important.

predict the probability a pixel would be classified as autumn olive. In both April and in June each model that detects and differentiates autumn olive from surrounding vegetation uses only a few features of the spectra: blue and red (480 and 710 nm in April, and 470 and 710 nm in June) reflectance. These regions demonstrate differentiability in not only the PLS-DA (Figures 4 and 5) but also in the spectral signatures (Figure 3).

In addition to developing an algorithm using the PLS-DA to differentiate autumn olive pixels from pixels of other plant species, a partial least squares regression (PLS-R) was also used. Wavelengths in the 450-550 nm, 650-700 nm, and 700-NIR regions are important for discrimination in both months (Figure 6A and B), which aligns with the mean spectral signal of autumn olive pixels (Figure 3).

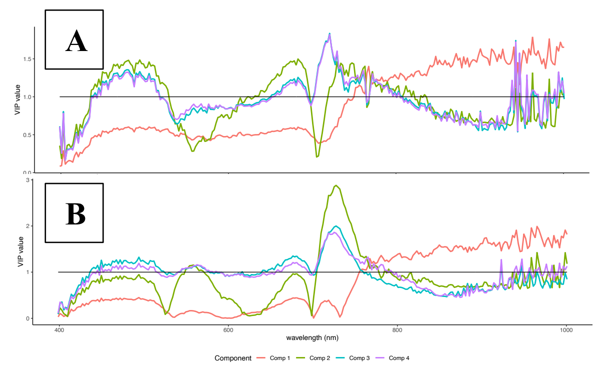

Figure 6. VIP values for first four components of PLS-R, which used reflectance across all wavelengths in autumn olive spectra to predict the probability a pixel would be classified as autumn olive in April (A) and June (B). Four components minimized error in classification; any more made for a less parsimonious model. VIP values above 1 (marked as a horizontal line) can be assumed to be important.

Model Results

Using the simple linear model produced from the PLS-DA of April data, the likelihood of false positives (falsely classifying individuals that are not autumn olive as autumn olive) is 0, but the likelihood of false negatives (falsely classifying individuals that are autumn olive as not autumn olive) is 64% (Figure 7A). Using the PLS-R to classify individuals in April produced better results: the likelihood of false positives remained 0, and the likelihood of false negatives was reduced to 18% (Figure 7B).

Using the simple linear model produced from the PLS-DA of June data, the likelihood of false positives is 0, but the likelihood of false negatives is 31% (Figure 7C). Using the PLS-R to classify individuals in June produced better results: the likelihood of false positives increased to 3%, but the likelihood of false negatives was reduced to 0% (Figure 7D).

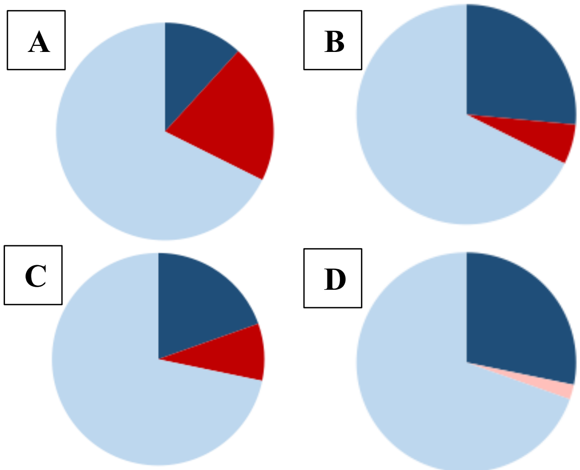

Figure 7. Results of classification accuracy using: PLS-DA and PLS-R models in April (A and B, respectively) and PLS-DA and PLS-R models in June (C and D, respectively). Dark blue represents true positives, light blue represents true negatives. Dark red represents false negatives, and pink represents false positives.

Discussion

Ability to detect autumn olive

The use of a PLS-DA, which classifies individuals into different groups using their reflectances at various wavelengths can elucidate patterns of inter- and intra-specific variability. The PLS-DA results, along with the mean spectral signatures by species demonstrate that intra-individual and intra-specific variability of autumn olive do not impede the ability to differentiate it.

The results of the linear models and PLS-R models both demonstrate the ability to detect autumn olive individuals within an image, particularly in June. While the PLS-R model is more accurate, the simple linear model, which significantly reduces computational demands and time, is also quite accurate and demonstrates potential for broader, open access applications.

Future Work

While the results thus far show a great deal of promise, we plan to continue comparing different classification approaches at different points in the growing season. Combining the results of classification over multiple dates also has the potential to maximize the effectiveness of detection. We also hope to extend our field-based leaf-scale algorithms for detection to datasets from the National Ecological Observatory Network to determine whether fine-scale resolution data are applicable to coarser resolution data and therefore application at the landscape scale.

The success of this project has widespread implications for the management of invasive species. There are potentially broad-reaching benefits, including expanding the techniques to larger spatial extents, which would enhance regional strategies for invasive plant management far beyond what can be done with ground surveys alone. Insights from this project have important implications for scientists in ecology and environmental sciences, forest and park services, and land owners managing invasive species on their property.

Acknowledgments

This project has benefited from Rod Walker at the Blue Ridge Program for Regional Invasive Species Management (PRISM) and Xi Yang at the University of Virginia, who each provided expertise on invasive plants and remote sensing, respectively. The initial portion of this project, in which protocols for data collection and analysis were established, was funded by a Conservation Innovation Grant from the United States Department of Agriculture Natural Resources Conservation Service. The faculty at Blandy Experimental Farm provided the field sites for data collection and continue to support this project, intellectually and financially. My parents Natalie and Steve Huelsman supported me through countless hours of drone maintenance and learning. My partner Cole Oberman has patiently allowed me to bring research equipment into our home for the last two years and has helped to solve many mechanical issues. My colleague Allie Parisien has provided countless hours of field site assessment, data collection, and moral support. Lastly, my undergraduate research assistants Nina Copeland, Emma Dereberry, Aline Johnson, Anthony Murphy-Neilson, Sidney Stephens, Lydia Mullori, Jenna Vance, Naomi Harris, and Davis Coffey have all helped with data analysis, inspired me to hone my research questions, and improved my scientific communication.

References

Aneece, I., Epstein, H., 2017. Identifying invasive plant species using field spectroscopy in the VNIR region in successional systems of north-central Virginia. International Journal of Remote Sensing 38, 100–122. https://doi.org/10.1080/01431161.2016.1259682

Asner, G., Vitousek, P., 2005. Remote analysis of biological invasion and biogeochemical change. Proceedings of the National Academy of Sciences of the United States of America 102, 4383–6. https://doi.org/10.1073/pnas.0500823102

Asner, G.P., Martin, R.E., 2008. Spectral and chemical analysis of tropical forests: Scaling from leaf to canopy levels. Remote Sensing of Environment 112, 3958–3970. https://doi.org/10.1016/j.rse.2008.07.003

Blackburn, G.A., 2007. Hyperspectral remote sensing of plant pigments. J Exp Bot 58, 855–867. https://doi.org/10.1093/jxb/erl123

Cardina, J., Johnson, G., Sparrow, D., 1997. The nature and consequence of weed spatial distribution. Weed Science 45, 364–373. https://doi.org/10.1017/S0043174500092997

Carson, H.W., Lass, L.W., Callihan, R.H., 1995. Detection of Yellow Hawkweed (Hieracium pratense) with High Resolution Multispectral Digital Imagery. Weed Technology 9, 477–483.

Castro, K., Sanchez-Azofeifa, G.A., Caelli, T., 2004. Discrimination of lianas and trees with leaf-level hyperspectral data. Remote Sensing of Environment 90, 353–372. https://doi.org/10.1016/j.rse.2004.01.013

Castro-Esau, K.L., Sánchez-Azofeifa, G.A., Rivard, B., Wright, S.J., Quesada, M., 2006. Variability in leaf optical properties of Mesoamerican trees and the potential for species classification. American Journal of Botany 93, 517–530. https://doi.org/10.3732/ajb.93.4.517

Chance, C.M., Coops, N.C., Plowright, A.A., Tooke, T.R., Christen, A., Aven, N., 2016. Invasive Shrub Mapping in an Urban Environment from Hyperspectral and LiDAR-Derived Attributes. Front Plant Sci 7. https://doi.org/10.3389/fpls.2016.01528

Clark, M., Roberts, D., Clark, D., 2005. Hyperspectral discrimination of tropical rain forest tree species at leaf to crown scales. Remote Sensing of Environment 96, 375–398. https://doi.org/10.1016/j.rse.2005.03.009

Cochrane, M.A., 2000. Using vegetation reflectance variability for species level classification of hyperspectral data. International Journal of Remote Sensing 21, 2075–2087. https://doi.org/10.1080/01431160050021303

Gaertner, M., Den Breeyen, A., Hui, C., Richardson, D., 2009. Impacts of alien plant invasions on species richness in Mediterranean-type ecosystems: a meta-analysis. Progress in Physical Geography 33, 319–338. https://doi.org/10.1177/0309133309341607

Gurevitch, J., Padilla, D.K., 2004. Are invasive species a major cause of extinctions? Trends Ecol Evol 19, 470–474. https://doi.org/10.1016/j.tree.2004.07.005

Hamilton, R., Megown, K., Lachowski, H., Campbell, R., 2006. Mapping Russian olive: using remote sensing to map an invasive tree.

Hochberg, E., Roberts, D., Dennison, P., Hulley, G., 2015. Special issue on the Hyperspectral Infrared Imager (HyspIRI): Emerging science in terrestrial and aquatic ecology, radiation balance and hazards. Remote Sensing of Environment 167. https://doi.org/10.1016/j.rse.2015.06.011

Kaufmann, H., Segl, K., Guanter, L., Hofer, S., Förster, K.-P., Stuffler, T., Müller, A., Richter, R., Bach, H., Hostert, P., Chlebek, C., 2008. Environmental Mapping and Analysis Program (EnMAP) - Recent Advances and Status. Presented at the International Geoscience and Remote Sensing Symposium (IGARSS), pp. 109–112. https://doi.org/10.1109/IGARSS.2008.4779668

Kganyago, M., Odindi, J., Adjorlolo, C., Mhangara, P., 2017. Selecting a subset of spectral bands for mapping invasive alien plants: a case of discriminating Parthenium hysterophorus using field spectroscopy data. International Journal of Remote Sensing 38, 5608–5625. https://doi.org/10.1080/01431161.2017.1343510

Kimothi, M.M., Dasari, A., 2010. Methodology to map the spread of an invasive plant (Lantana camara L.) in forest ecosystems using Indian remote sensing satellite data. International Journal of Remote Sensing 31, 3273–3289. https://doi.org/10.1080/01431160903121126

Mahlein, A.-K., Steiner, U., Dehne, H.-W., Oerke, E.-C., 2010. Spectral signatures of sugar beet leaves for the detection and differentiation of diseases. Precision Agric 11, 413–431. https://doi.org/10.1007/s11119-010-9180-7

Martin, M.E., Aber, J.D., 1997. High Spectral Resolution Remote Sensing of Forest Canopy Lignin, Nitrogen, and Ecosystem Processes. Ecological Applications 7, 431–443. https://doi.org/10.1890/1051-0761(1997)007[0431:HSRRSO]2.0.CO;2

Matongera, T., Mutanga, O., Lottering, R., 2016. Detection and mapping of bracken fern weeds using multispectral remotely sensed data: A review of progress and challenges. Geocarto International 33, 1–31. https://doi.org/10.1080/10106049.2016.1240719

Mutanga, O., Skidmore, A.K., Prins, H.H.T., 2004. Predicting in situ pasture quality in the Kruger national Park, South Africa, using continuum removed absorption features. REMOTE SENS ENVIRON 89, 393–408. https://doi.org/10.1016/j.rse.2003.11.001

Palmer, M.W., Earls, P.G., Hoagland, B.W., White, P.S., Wohlgemuth, T., 2002. Quantitative tools for perfecting species lists. Environmetrics 13, 121–137. https://doi.org/10.1002/env.516

Peerbhay, K., Mutanga, O., Lottering, R., Bangamwabo, V., Ismail, R., 2016. Detecting bugweed (Solanum mauritianum) abundance in plantation forestry using multisource remote sensing. ISPRS Journal of Photogrammetry and Remote Sensing C, 167–176. https://doi.org/10.1016/j.isprsjprs.2016.09.014

Rocchini, D., Chiarucci, A., Loiselle, S., 2004. Testing the spectral variation hypothesis by using satellite multispectral images. Acta Oecologica 26, 117–120. https://doi.org/10.1016/j.actao.2004.03.008

Sanchez-Azofeifa, G.A., Calvo-Alvarado, J., Espírito-Santo, M., Fernandes, G., Powers, J., Quesada, M., 2013. Tropical Dry Forests in the Americas: The Tropi-Dry Endeavor. pp. 1–16.

Schmidt, K.S., Skidmore, A., 2003. Spectral discrimination of vegetation types in a coastal wetland. Remote Sensing of Environment 85, 92–108. https://doi.org/10.1016/S0034-4257(02)00196-7

Skowronek, S., Ewald, M., Isermann, M., Van De Kerchove, R., Lenoir, J., Aerts, R., Warrie, J., Hattab, T., Honnay, O., Schmidtlein, S., Rocchini, D., Somers, B., Feilhauer, H., 2017. Mapping an invasive bryophyte species using hyperspectral remote sensing data. Biological Invasions 19, 239–254.

Thenkabail, P.S., Gumma, M.K., Teluguntla, P., Mohammed, I.A., 2014. Hyperspectral Remote Sensing of Vegetation and Agricultural Crops. Photogrammetric Engineering & Remote Sensing (PE&RS) 80, 697–723.

Ustin, S.L., Roberts, D.A., Gamon, J.A., Asner, G.P., Green, R.O., 2004. Using Imaging Spectroscopy to Study Ecosystem Processes and Properties. BioScience 54, 523–534. https://doi.org/10.1641/0006-3568(2004)054[0523:UISTSE]2.0.CO;2

Xiao, Y., Zhao, W., Zhou, D., Gong, H., 2014. Sensitivity Analysis of Vegetation Reflectance to Biochemical and Biophysical Variables at Leaf, Canopy, and Regional Scales. Geoscience and Remote Sensing, IEEE Transactions on 52, 4014–4024. https://doi.org/10.1109/TGRS.2013.2278838